We are IntechOpen, the world's leading publisher of Open Access books Built by scientists, for scientists

4,800
Open access books available

122,000
International authors and editors

135M
Downloads

Our authors are among the

154
Countries delivered to

TOP 1%
most cited scientists

12.2%
Contributors from top 500 universities

CLARIVATE ANALYTICS BOOK CITATION INDEX INDEXED

WEB OF SCIENCE™

Selection of our books indexed in the Book Citation Index in Web of Science™ Core Collection (BKCI)

Interested in publishing with us?
Contact book.department@intechopen.com

Numbers displayed above are based on latest data collected.
For more information visit www.intechopen.com

Chapter 1

Atomic Force Microscopy Observations of the Polymer Network Structure Formed in Ferroelectric Liquid Crystals Cells

M. Petit

Additional information is available at the end of the chapter

http://dx.doi.org/10.5772/46095

1. Introduction

Polymer network stabilized liquid crystals (PSLCs) have attracted increasing interest over the past decade because of their potential applications mainly in electro-optic devices such as displays and light shutters [1-5]. The main motivation to incorporate a polymer network in liquid crystal cells was to bulk-stabilize a desired director configuration against any mechanical shock and distortions which can irreversibly alter the functionality of the cells. The PSLCs are composite materials in which a low density polymer network is dispersed within liquid crystal medium [6,7]. The polymer network is formed by chemical crosslinking of a small amount (few percent) of photo-reactive monomers dissolved in low molecular weight mesogenic material, through a polymerization reaction photochemically activated by a UV illumination. When the polymerization occurs in an aligned geometry, the resulting polymer network is roughly aligned parallel to the direction initially imposed by the liquid crystal medium in which the network has been formed [8]. Depending on the type of the reactive mesogen, the morphology of the polymer network may correspond to an open structure consisting of anisotropic fibrils [8-10]. The lateral size of fibrils is of the order of a few tenths of a micron [11-13]; their density increases with the initial reactive monomer concentration. The polymer fibrils, by creating a large internal boundary, provide a bulk anchoring mechanism which allows a control of the liquid crystal alignment in the bulk. Application of an electric field causes a distortion of the liquid crystal host, which corresponds to a field-induced director rotation, without any reorientation of the fibrils [8] considered rigid by the authors because the network is heavily cross-linked. The structure of the polymer network has been observed using different techniques. The scanning electron microscope (SEM) observations, observations between crossed polarizer after removal of the un-reacted species and observations at high temperature, all provide information on the

network structure. The SEM and crossed polarizers observations give a detailed of the lateral size of fibrils [11-13] and the width of the fibers. Most of these observations have been reported in the nematic [14] or cholesteric [15] liquid crystals phases. However, a few information has been reported in the literature about the vertical distance between fibers especially when the polymer network was formed in a ordering helical ferroelectric liquid crystals (SmC*) and paraelectric SmA phases (PSFLC). The PSFLC composites have been investigated by different methods, electro optic technical [16-22] and dielectric method [23-26]. It is know that the dielectric properties of the ferroelectric liquid crystals in the ideal unbounded sample are nowadays well understood. The dielectric dispersion is essentially dominated by the dynamic of the soft mode, responsible for the phase transition from the paraelectric phase SmA to the ferroelectric phase SmC* phase, and the Goldstone mode connected with the helical structure in the ferroelectric SmC* phase [27]. The subject is already compiled in monographs [28,29].

Detailed dielectric spectroscopic study over a wide temperature and frequency ranges in the PSFLC systems reveal different molecular dynamics of this type of composites [23-25]. It was reported [23-25], that the dielectric strength of the Goldstone mode decreases with increasing polymer concentration, however, the relaxation frequency was found to be higher for the PSFLC composite film compared to that of the corresponding pure FLC. However, the behavior of the soft mode dielectric strength is not completely explained yet. Kundu et al. [25] are showed for polymer stabilized ferroelectric liquid crystal (PSFLC) systems that the soft mode dielectric strength remains unchanged when the FLC cells are stabilized by a polymer network formed from a nonmesogenic reactive monomer. The most of these studies have not given a quantitative interpretation of the dielectric response until our work published in [26].

In our previous study [26], although the range of the SmA phase is very narrow, the effect of the polymer network on the soft mode is clearly observed. By increasing the polymer concentration the dielectric strength is reduced and the relaxation frequency is increased [26].

It is knows that, in a thin enough sample when the sample thickness becomes comparable with the pitch of the helix, the entire structure in helix-free. The director twist-bend fixed by the surface polar anchoring can still exist as well as in the helicoidal samples. This spaced modulation is called a twisted structure [30]. However when the twist helical pitch is confining with the polymer network in a thin thickness, logically there is no reason that the twisted structure still remains in spite of the confinement effects. In this chapter we will illustrate that in spite of the confinement of the twist short helical structure in a polymer network the ferroelectric liquid crystal conserves the helical structure. This behavior was interpreted by the type of the morphology of the polymer network which is formed in the liquid crystals medium. After describing the dielectric responses, in sect.3-2-A we will describe in detail the effect of the polymer network density formed in a planar alignment of the ferroelectric liquid crystals cells [30] on the dielectric responses namely soft and Goldstone mode. The results of the dielectric responses were interpreted by the morphology of the polymer network using atomic force microscopy investigations. In sec.3-2-B the effect of the applied electric field during the photopolymerisation on the dielectric responses is

reported, the observations of the structure of the polymer network by AFM agree well with all dielectric responses.

2. Experiments

The liquid crystal compound used in these studies is the ROLIC 8823 (Rolic research ltd) which exhibits the following phase sequence: Crystal (Cr) -27 °C SmC* 63.5 °C SmA 65°C Isotropic (Figure 1). In the SmC* phase (Figure 2), at low temperature the helical pitch is about 0.3µm and the spontaneous polarization (P_s is close to 100 nC/cm²). To prepare the polymer network we have used a photoreactive diacrylate mesogen as photocurable monomer which presents a nematic (N) phase between Cr and Isotropic phases Cr−88 °C−N−118 °C− Isotropic. The chemical structure of the monomer is presented in figure 3.

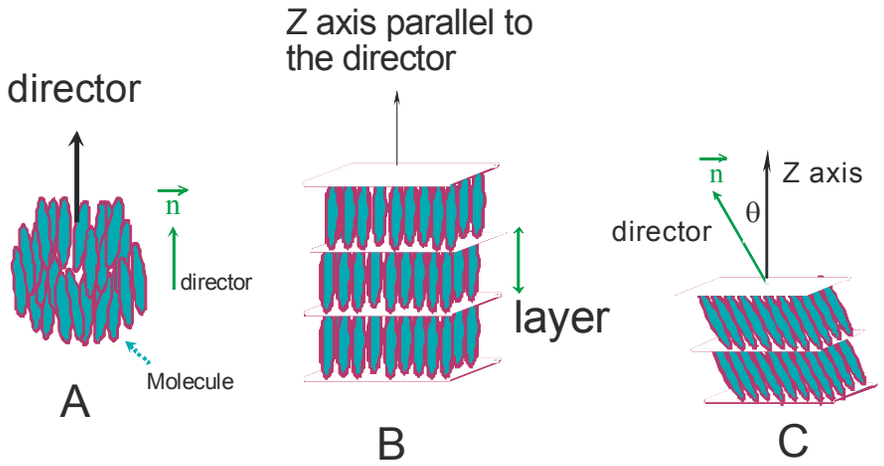

Figure 1. A schematic representation of the nematic phase (A), Paraelectric phase or smectic A (B) and Smectic C (C).

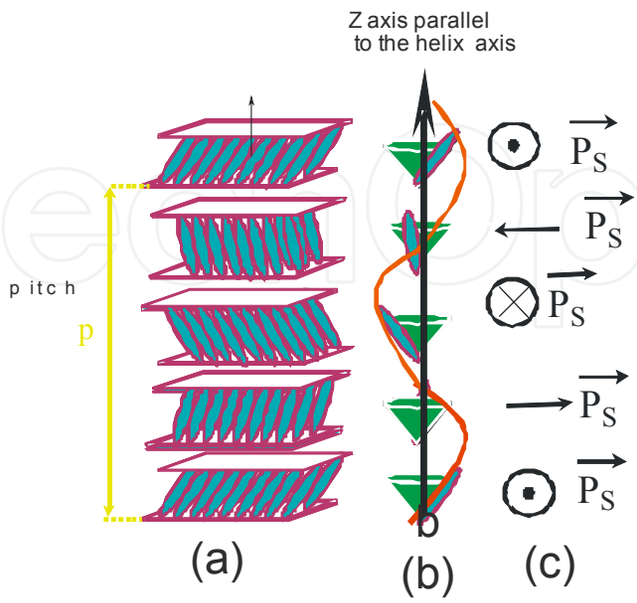

Figure 2. A schematic representation of a smectic C* phase : molecular order in the layer (a), helical structure (b) and the direction of the ferroelectric spontaneous polarization in the smectic layers planes (c).

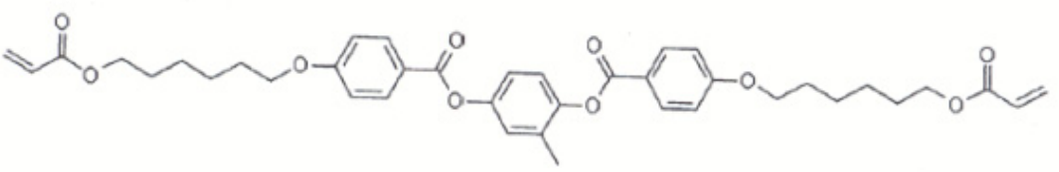

Figure 3. The molecular structure of the monomer.

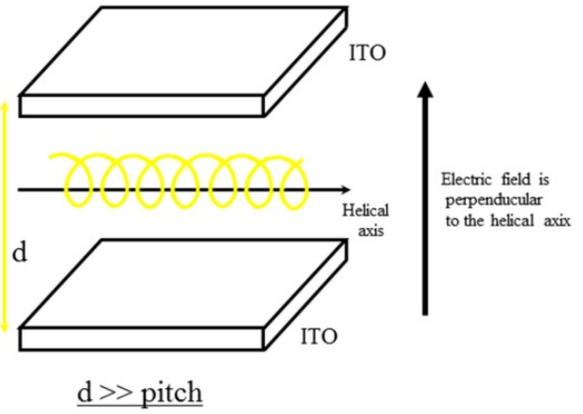

Figure 4. The Planar configuration of the helical structure in our system, the electric field is applied perpendicular to the helical axis.

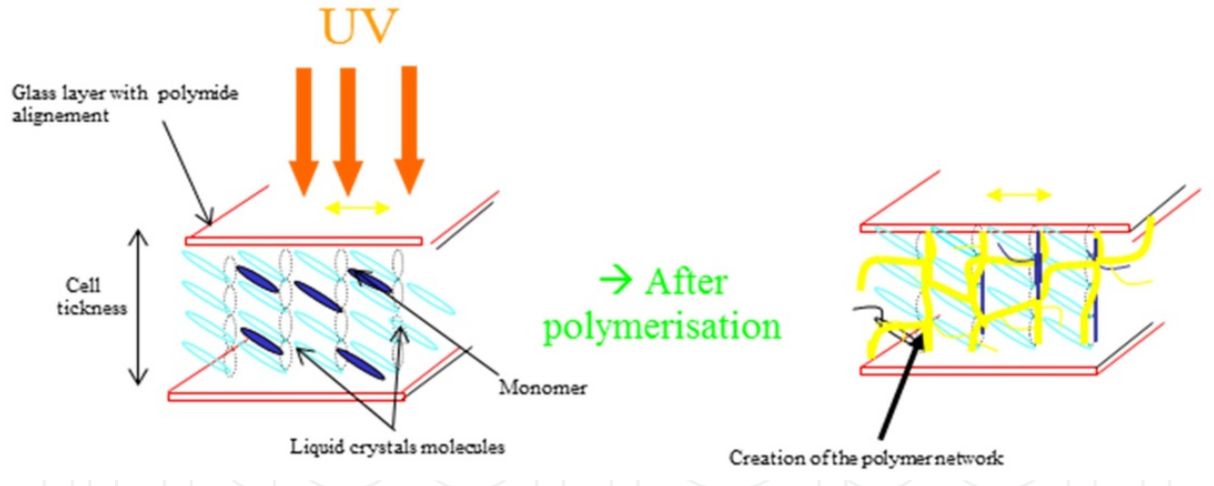

Figure 5. A schematic illustration the formation of the polymer network, before de photopolymerisation (on the left) and after the pohopolymerisation (on the right).

The PSFLC mixture was prepared by mixing the Diacrylate monomer with weight concentrations between 2 and 7%. The ferroelectric liquid crystals (FLC) compound and the diacrylate were dissolved in the isotropic phase to make a homogeneous mixture. A 5 μm thick EHC Inc, Japon-cell (two glass faces were treated with polyimide to favorite a planar alignment (Figure 4)) was filled by the mixture in its isotropic phase. In order to obtain a good alignment in the SmC* phase, the cell was slowly cooled (0.1 °C/minute) from the isotropic phase under an applied electric field (5V/μm) into the SmC* phase. For the section

3.2.A, the sample cells were then exposed to ultraviolet light (wavelength λ = 365nm) at 25 °C with an intensity of 5 (mW/cm²) for 30 minutes without any applied electric field. Here, polymer phase separation and network formation take place (Figure 5). During these studies, the cell was placed on a hot stage (Linkam TMS 93) for temperature control. The texture observations of the cells were carried out by means of a polarized optical microscope (POM)(LEICA DMRXP).

Dielectric measurements were performed in the frequency range of 10 Hz–13 MHz HP 4192A. In a linear dielectric response, the time dependent polarization $P(t)$ of the sample, being induced by a weak measuring electric field $E(t)$, is proportional to the field :

$$P(t)= \varepsilon_0 (\varepsilon^*-1) E(t) \text{ where } E(t)=E_0 exp(-i\omega t)$$

Is a sinusoidal electric field applied to the dielectric under test and ε^* is the complex dielectric permittivity, ω is the angular frequency, and f is the frequency of measuring electric field displayed in the channel A of most impedance analyzers, and ε_0 is the dielectric permittivity of free space. In linear dielectric spectroscopy the amplitude of the measuring electric field should be chosen so that it does not suppress the helicoidal structure of the SmC* phase. Generally for ferroelectric liquid crystals two processes contribute to the dielectric spectra. We are interesting here only to the collective processes namely soft and Goldstone modes.

In order to obtain the characteristic dielectric strengths and relaxation frequencies of the ferroelectric relaxation modes, the dielectric spectra were fitted simultaneously by the Cole-Cole function :

$$\varepsilon^* = \varepsilon_\infty + (\Delta\varepsilon_G) / (1+jf/f_G)^{1-\alpha_G} + (\Delta\varepsilon_s) / (1+jf/f_s)^{1-\alpha_s} + (\sigma/j2\pi f\varepsilon_0) \quad (1)$$

Where f is the frequency, ε_∞ is the high frequency limit of the dielectric permittivity, $\Delta\varepsilon_G$ and $\Delta\varepsilon_s$ represent the dielectric strengths corresponding to Goldstone and soft modes, respectively ; f_G and f_s represent the relaxation frequencies of the two modes, α_G and α_s are the distribution parameters, and σ is the electric conductivity. The temperature dependencies of different dielectric processes are reported and discussed below. To image the topography of polymer networks a Veeco Multimode Atomic Force Microscopy (AFM) equipped with a Nanoscope IIIa controller was used. All AFM scans were taken in tapping mode with commercially available tips made of Phosphorus doped Silicon.

3. Results and discussion

3.1. Optical observations

The first objective of this study was to investigate the effect of the applied electric field and phase order (before the polymerization) on the alignment on the polymer network formed in the FLC host. To illustrates the effect of the applied electric field during the cooling from the isotropic phase to the SmC* phase on the alignment of the SmC* layers we present on Figure 6.

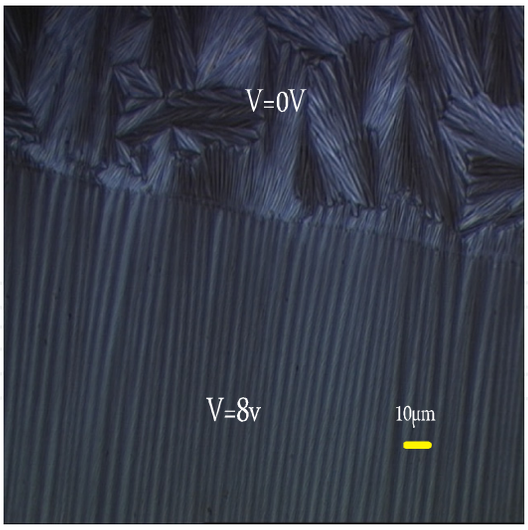

Figure 6. Optical micrographs of PSFLC samples obtained between crossed polarizers at T = 70 ◦C, for 7% polymer concentrations formed at 25°C. (V=0V) indicate the region where no field was applied and (V=8 v) indicate the region where an electric field was applied.

Figure 6 shows example of optical micrographs representing the observed textures of the PSFLC cells obtained for 7% initial monomer concentration. These micrographs were obtained at a temperature of 70 ° C (above the SmA- Isotrope transition temperature) so that only the birefringence associated to the polymer network would appear. The micrographs of Figure 6 clearly show the anisotropic structure of the polymer network. The optical observation of this anisotropic structure is due not only to the residual birefringence of polymer fibrils, but also to the remaining birefringence of the surrounding FLC molecules which are still aligned by the polymer structure. Two regions have been observed (Figure 6), the first region when no electric field has been applied (V=0V), the polymer network was randomly distributed. However, in the region where an electric field is applied (V=8V) the polymer network presents a good alignment. To illustrate the effect of the phase order on the formation of the polymer network, two cells of 7% polymer concentration were polymerized in two different temperatures. The first cell was polymerized at 25°C. The measured helical pitch at 25°C is about 0.25 μm (Figure 7). However, the second cell was polymerized at high temperature (T=58°C) where the helical pitch diverges (Figure 7). Figure 8 shows the optical micrographs representing the PSFLC cells obtained for 7% polymer concentration which are polymerized at two different temperatures. As seen in this figure, the dechiralisation lines [31] have been clearly observed on the structure of the polymer network (dechiralisation lines are perpendicular to the polymer fibers (Figure 8 (a))).

We can remember here, that the dechiralisation lines are well known lines defects can be observed in a planar samples filled by a highly twisted FLC [30-32]. In a smectic C* sample, competition between a strong surface anchoring and a helicoidal configuration in the bulk induces a double lattice of singular lines. These lines are located near both the boundary surfaces and are parallel to the plane of the layers [30-32]. Those lines are named the dechiralisation lines. Hence, these results illustrate that the polymer structure conserves locally a lines defect print. We can also indicate here that the fact that the helical structure of the FLC at T=25°C is very shorter no twisted structure on the polymer fiber has been

observed by polarizing microscopy. However, when the polymer network was formed at high temperature, the helical structure of the polymer fibers is easy observed by polarizer microscopy (Figure 8 (b)). One can seen that, at high temperature, the dechiralisation lines were not printed on the polymer fibers. That illustrate that the order and structure of the liquid crystal phase are transferred onto the polymer network. It has been already shown by Archer et al [33] that the defect of the FLC twisted grain boundary were found printed on the polymer network structure. However, for short-pitch ferroelectric liquid crystals, the transfer of the lines defects has not been observed. Figure 8 shows also that the polymer network which was formed at high temperature, the dechiralisation lines were not printed on the polymer fibers. Because, when approaching the phase transition SmC*- SmA, the helical pitch diverges. The divergence of the helical pitch (unwinding of the helix) is seen as disappearance of dechiralisation lines [31].

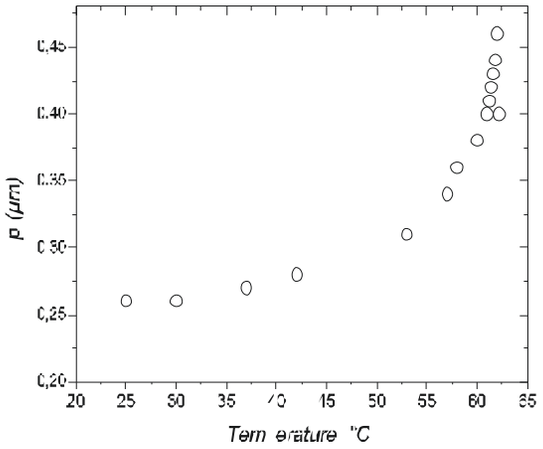

Figure 7. Temperature dependence of the helical pitch of the FLC measured by mean of Grandjean-Cano method [32].

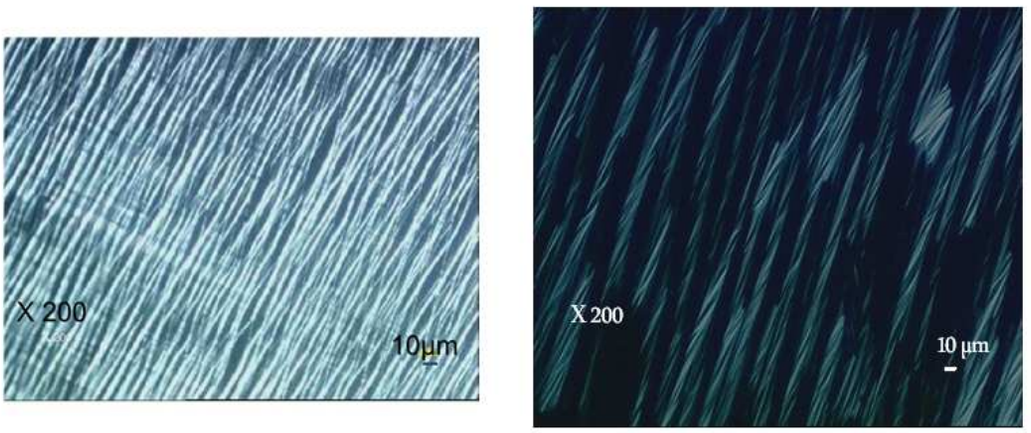

(a) (b)

Figure 8. Optical microscopy images between crossed polarizers at T = 70 ◦C, for 7% polymer concentration. (a) polymerization at 25°C (dechiralisation lines are clearly observed and correspond to the straight lines which are perpendicular to the polymer fibers). (b) polymerization at 58°C (the polymer fibers present a helical structure).

This implies that even after polymerization, the characteristic property of the host phase in which polymerization was carried out was effectively retained.

3.2. Dielectric studies

3.2.1. Effect of the polymer network density on the dielectric responses

*Goldstone mode of the SmC**

Figures 9 (a) and (b) show examples of the dispersion, $\varepsilon'(f)$ and absorption, $\varepsilon''(f)$ dielectric spectra obtained in the SmC* phase at low temperatures for different polymer concentrations. For all of the concentrations studied, two relaxation mechanisms were detected. The first, at low frequencies between (1 and 3 kHz) with a high amplitude, is due to the Goldstone mode; whereas the second observed at high frequencies (> 1 MHz) with a weak amplitude is an artifact due to the indium tin oxide (ITO) conducting layers. As shown in Fig. 9(a), at low frequencies, the dielectric response shows a very strong polymer concentration dependence; at 100 Hz, for example, $\varepsilon'(f)$ decreases from 100 to 30 when the polymer concentration increases from 0% to 7%.

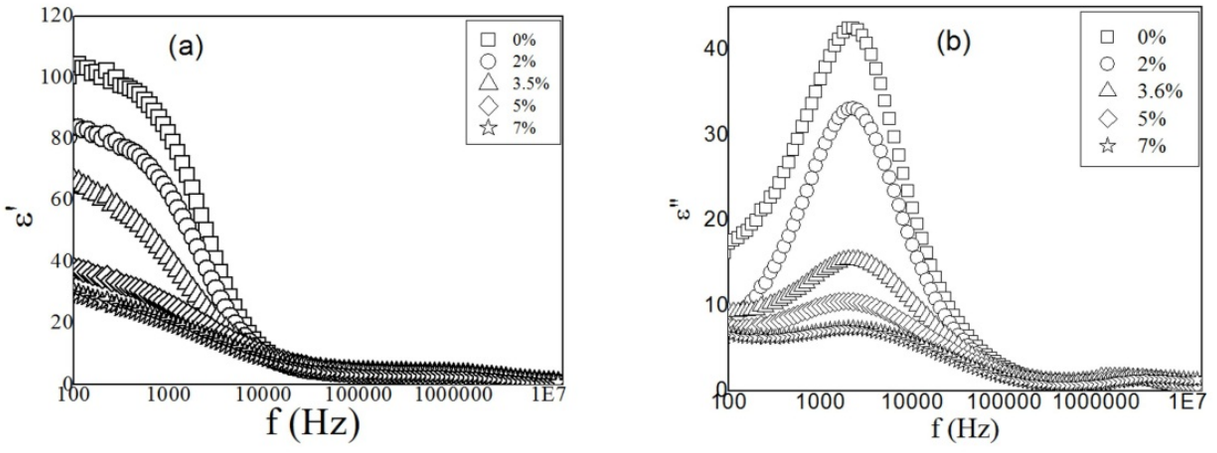

Figure 9. Frequency dependence of (a) the real and (b) the imaginary parts of complex permittivity in the smectic C* phase for different poclymer concentrations at T=25 °C.

This effect is also clearly illustrated in the behavior of the absorption peak observed in the $\varepsilon''(f)$ spectra [Fig. 9 (b)]; the absorption peak strongly decreases from 48 to 8 when the polymer concentration is varied from 0% to 7%. The parameters $\Delta\varepsilon_G$ and f_G obtained from the curve-fit procedure are displayed in Figs. 10 (a) and (b). The behavior of $\Delta\varepsilon_G$ versus temperature showed the same general features for all the samples Fig.10 (a) ; $\Delta\varepsilon_G$ slightly increases to reach a maximum at a temperature called T_{max} 3 °C below T_c then decreases abruptly above T_{max}. The behavior of $\Delta\varepsilon_G$ versus temperature is dependent on that of the helical pitch of the FLC Fig. 7. Usually the maximum observed in $\Delta\varepsilon_G(T)$ is related to that exhibited by the helical pitch Fig. 7 at temperatures close to T_c and indicates that the helical structure of the FLC is preserved in all our PSFLC systems.

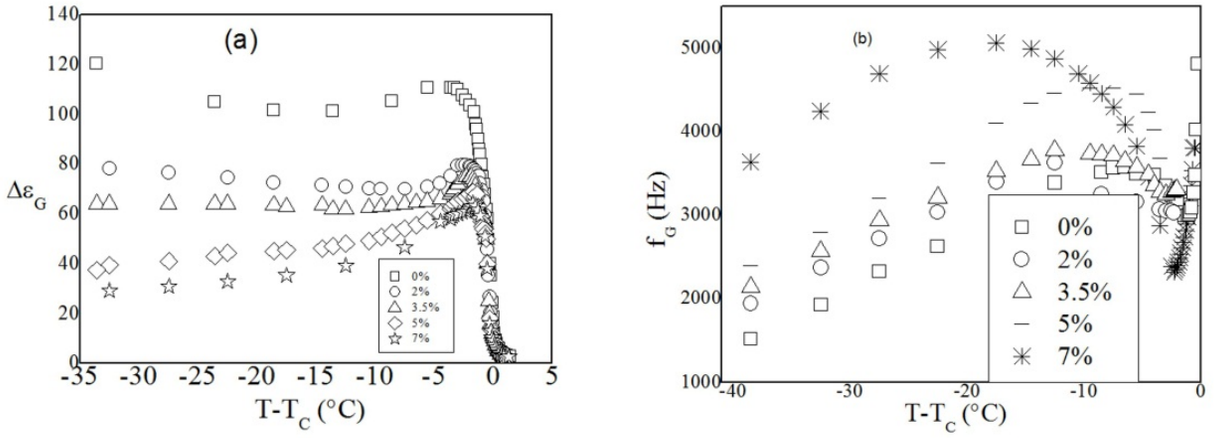

Figure 10. Temperature dependence (a) of $\Delta\varepsilon_G$ and (b) the relaxation frequency of the Goldstone mode for different polymer concentrations.

The temperature dependence of the Goldstone relaxation frequency Fig. 10 (b) shows that f_G slightly increases with temperature, reaches a maximum, and then rapidly decreases to a minimum value at a temperature corresponding to T_{max}, after T_{max}, an abrupt increase in f_G is observed for a temperature close to T_c. Qualitatively, the thermal behavior of the Goldstone mode is not affected by the polymer network. However, quantitative differences were observed for $\Delta\varepsilon_G$ and f_G when the polymer network density increases. To illustrate this effect, we present on Figs. 11 (a) and 11 (b) the evolution at room temperature of $\Delta\varepsilon_G$ and f_G as a function of the polymer concentration. It can be seen from these figures that the increase in the polymer concentration from 0% to 7% leads to a breakdown of $\Delta\varepsilon_G$ from 120 to 27 and to an increase in f_G from 1.5 to 3.5 kHz. Changes in the dynamic of the Goldstone mode have already been observed in PSFLC systems by Gasser et al. [35] and in other composite based FLC, as a random network formed from dispersions of aerosil particles within FLC media [36–38]. For aerosil/FLC composites, a decrease in $\Delta\varepsilon_G$ and a shift of f_G toward high frequencies [37,38] with increasing the density of aerosol particles were observed.

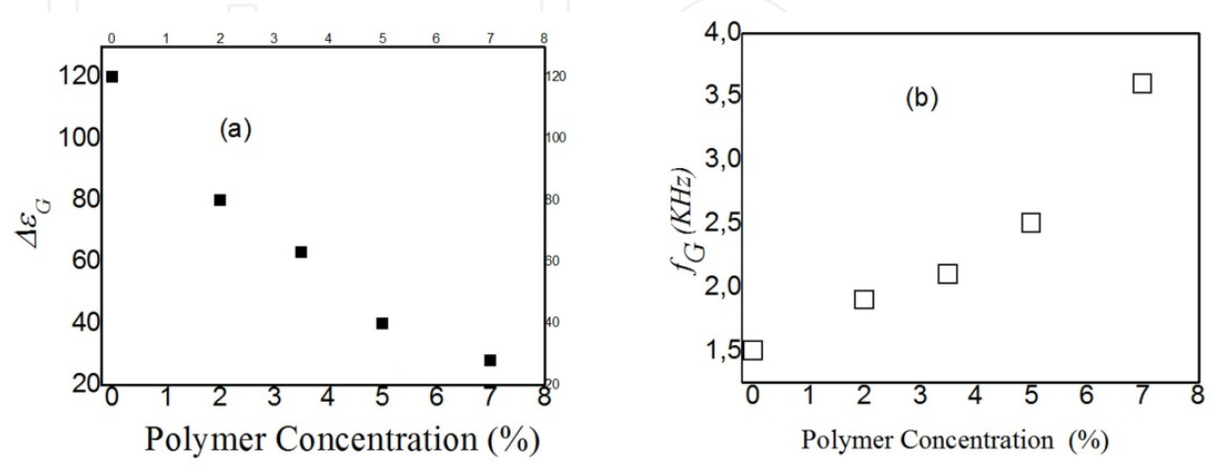

Figure 11. The dielectric strength ($\Delta\varepsilon_G$) (a) and relaxation frequency f_G (b) of the Goldstone mode at 25°C as function of the polymer concentration

The Goldstone mode even disappears in these systems for a sufficiently high aerosil density. The authors have interpreted the behavior of the dielectric response in these systems by size effects on smectic domains [36–38]; the reduction in the Goldstone mode strength and the increase in the relaxation frequency with increasing the concentration of aerosil particles are due, according to these authors, to the formation of smaller smectic domains where fluctuations are quenched by surface interactions, leading to a deformation of the helix. Additionally, the orientation of these smectic domains becomes randomly distributed so that fewer domains are therefore preferentially oriented in the direction of the applied electric field. We believe that the interpretation given above cannot explain the behavior of our PSFLC systems, despite similar changes in dielectric relaxation being observed. First, the polymer network in PSFLC cells are anisotropic and stabilizes the configuration of smectic domains oriented preferentially to the direction of the electric field. We think that the changes observed in dielectric response in our systems are essentially governed by elastic effects. We expect that the network-FLC interactions enhance the apparent elasticity of the PSFLC films, and accordingly, causes the increase in the relaxation frequency f_G and the reduction in dielectric strength $\Delta\varepsilon_G$. In fact, the dielectric strength and the relaxation frequency of the Goldstone mode in the case of a pure SmC* phase are expressed as [39] :

$$\Delta\varepsilon_G = (P_s/\theta)^2 / (2\varepsilon_0 K_\varphi q^2_0) \quad (2)$$

$$f_G = (K_{eff}\, q^2_0) / (2\pi\gamma_\varphi) \quad (3)$$

where γ_φ is the rotational viscosity, K_{eff} is the effective elastic constant. θ and P_s are the tilt angle and spontaneous polarization, respectively. $q_0 = 2\pi/p_0$ with p_0 is the helical pitch of the FLC. If we think that the Equations (2) and Equation (3) are applicable for the PSFLC composite, q_0 is considered here constant. The reduction in $\Delta\varepsilon_G$ as a function of polymer concentration is attributed to the variation in (P_s/θ) and/or K_{eff}. To clarify that, we have plotted in Fig. 12 the ratio (P_s/θ) as a function of polymer concentration. This figure shows that this ratio can be considered independent of the polymer concentration. As a consequence, the observed decrease in the $\Delta\varepsilon_G$ with polymer concentration can be explained rather by the increase in the effective elastic constant K_{eff}.

On the other hand, the relaxation frequency of the Goldstone mode Equation 3 is controlled both by the elastic ($K_{eff}\, q^2_0$) and viscous (γ_{eff}) forces. From the equation 3, the increase in f_G with polymer concentration can be explained by the decrease in the Goldstone rotational viscosity (γ_{eff}) and/or the increase in the effective elastic constant K_{eff}. From Eqs. 2 and 3, the effective rotational viscosity can be expressed as $(\gamma_{eff}) = (P_s\, \theta^{-1})^2 / 4\pi\varepsilon f_G\, \Delta\varepsilon_G$. According to this expression and using the experimental data of ($\Delta\varepsilon_G$ x f_G) (Fig 13(b)) and (P_s/θ) (Fig 12), γ_{eff} was evaluated as a function of temperature for all polymer concentrations studied. Generally, γ_{eff} of the PSFLC films increases with the polymer network density. At room temperature, for example, γ_{eff} increases from 0.2 to 0.6 *Pa. s* when the polymer concentration increases from 0% to 7% (Fig. 13(b)).

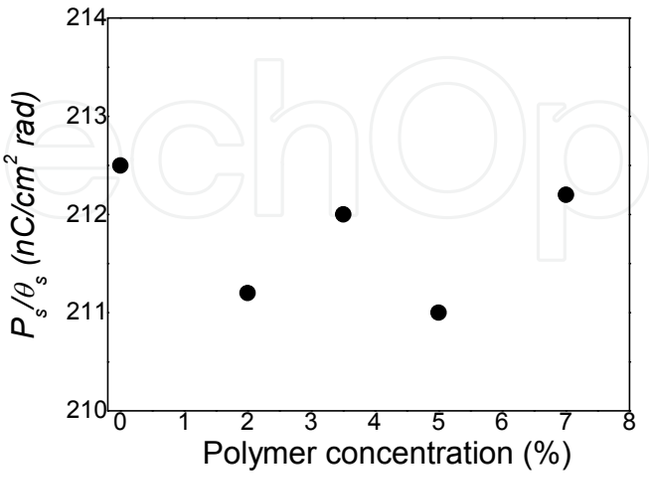

Figure 12. The (P_s/θ) ratio as function of the polymer network density

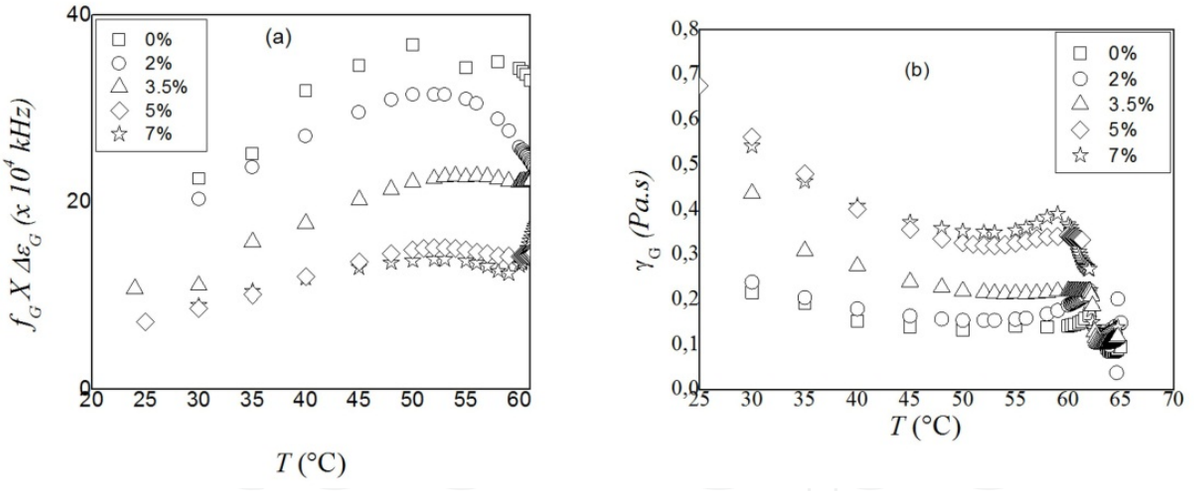

Figure 13. Temperature dependence of the Goldstone mode rotational viscosity (γ_{eff}) (b) and the product $\Delta\varepsilon_G$ x f_G (a) for different polymer concentrations.

Consequently, the increase in the relaxation frequency with the network density is certainly due to the increase in the effective elastic constant K_{eff}. To illustrate this, K_{eff} was evaluated at room temperature from Eqs. 2 and 3; the results are displayed in Fig. 14. This figure shows that K_{eff} linearly increases from 0.5 10^{-11} to 2.10^{-11} **N** when the polymer concentration increases from 0% to 7%. The values of K_{eff} found here compare well with those obtained for the same PSFLC systems from the electro-optic measurements [18,20].

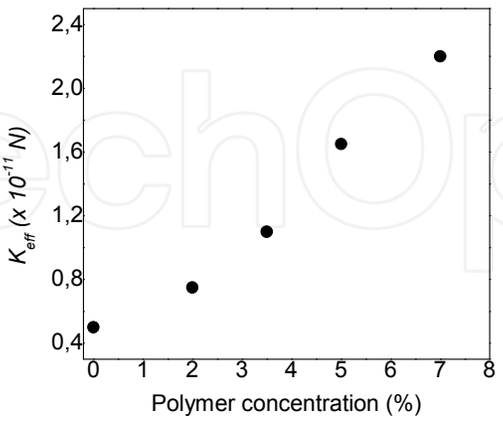

Figure 14. The effective twist elastic constant K_{eff} versus polymer concentration.

In conclusion, the increase in the relaxation frequency and the reduction in the dielectric strength of the Goldstone mode for the PSFLC films seem to be due to the increase in the twist elastic energy, resulting from the strong interaction between liquid crystal molecules and the polymer network liquid crystal molecules and the polymer network.

Polymer network morphology by AFM investigations:

The principal result surprising in this party (section 3-2-A) is the role played by a polymer network to stabilize of the ferroelectric order. Indeed Bayth et al [34] which are reported that when the helical pitch of the smectic C* was confined between two parallel glass with a homogeneous planar anchoring causes an unwound of the helical structure which is proportional to the cell thickness. This transition is due to the result of the competition between the energy cost of the lines of dechiralisation slightly dependent on the thickness and that to the unwound of helix which is highly depends to the cell thickness. A similar mechanism could be compared in the case of our results by schematizing the fibril like cylinders with a homogeneous planar anchoring along their axis. In this case, the work which is reported by Baytch et al should remain valid once subsisted the thickness of the cell by the distance between cylinders. We think that the fibril seem to have a twisted morphology. In this case, these morphology could stabilizes the smectic phase. The increase of the apparent elasticity coefficients can be explained from a simple energetic argument if we take into account the polymer network morphology. One must note here that the polymer network was formed within the SmC* phase in which the director field is highly twisted in a helix. This helical structure of the FLC is transferred on the polymer network as shown in Figure 15.

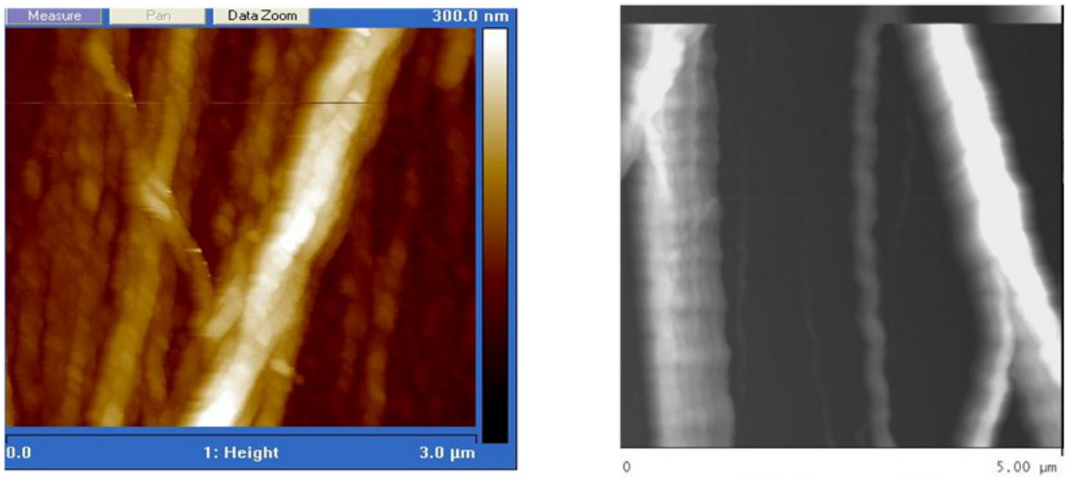

Figure 15. Tapping mode AFM height image of polymer fibers formed from a 5% polymer concentration into the short-pitch FLC (at T= 25°C). The twisted structure of fibrils is clearly observed indicating that the helical structure of the FLC from which the network was formed is printed on the polymer fibers.

For AFM experiments, the PSFLC cells were disassembled and flushed with solvent to remove the FLC. Figure 15 (on the left) presents a tapping mode AFM image (Veeco Instrument Inc.) of a 3×3 μm^2 region, and shows a fibrillar structure of the polymer network. The width of the fibers ranges from 150 to 300 nm. The AFM images clearly reveal a twisted structure of the fibers with a periodicity of about 0.24 μm which approximately corresponds to the pitch of the FLC helix used in this study. Hence, the polymer structure conserves locally a helical print which in turn stabilizes the FLC structure present during the polymerization. It has been already shown by I. Dierking et al. [12], and by G.A. Held et al.[40] that for long-pitch cholesteric liquid crystals, the helical superstaructure was transferred onto a polymer network. However, for short-pitch ferroelectric liquid crystals, this transfer has not been observed. Recently, K. Akagi et al [41] were confirmed the possibility of the printing of the short helical pitch on the polymer network. Archer et al [33] showed that the defect of the FLC twisted grain boundary were found printed on the polymer network structure. In [21] the chevron pattern has been observed on the polymer network. The printing of the helical structure on the polymer network is also reported by [42]. One could not observe any twisting of the polymer strands when polymerized in the Sm A* phase [43]. This implies that even after polymerization, the characteristic property of the host phase in which polymerisation was carried out was effectively retained. The helical aspect of the fiber structure certainly influences and explains the electro-optical: Deformed Helix ferroelectric liquid crystals (DHF) [18] and electroclinic effects [19,20].

Sof mode in the SmA phase

Figures 16 (a) and 16 (b) show examples of the dispersion, $\varepsilon'(f)$ and absorption, $\varepsilon''(f)$, dielectric spectra obtained in the SmA phase at T_c for each polymer concentration. Two relaxations mechanisms are detected. The first, at frequencies between 10 and 30 kHz

with a weak strength, is attributed to the soft-mode relaxation mechanism; whereas the second observed at high frequencies 1 MHz is due to the ITO conducting layers. As shown in Fig.16, at 1 kHz frequency, the dielectric response shows a very strong polymer concentration dependence; ε' decreases from 23 to 12 when the polymer concentration increases from 0% to 7%. This effect is also clearly demonstrated from the behavior of the absorption peak observed in Fig. 16 (b); the absorption peak decreases from 12 to 3 when the polymer concentration is varied from 0% to7%. We present in Figs. 17 (a) and 17 (b) the temperature dependence of the dielectric strength, $\Delta\varepsilon_s$, and the relaxation frequency, f_s, of the soft mode. For all studied concentrations, the behavior of versus temperature shows the same general features fig. 17 (a). A rapid increase in $\Delta\varepsilon_s$ is observed close to T_c for all concentrations studied. The increase in $\Delta\varepsilon_s$ at and close to T_c is dependent on the polymer concentration. Note that $\Delta\varepsilon_s$ becomes relatively weakly affected by the network as temperature increases from T_c (Fig. 17 (a)). The relaxation frequency, f_s, exhibits a linear temperature dependence (Fig. 17 (b)). At T_c, f_s increases from 10 to 36 kHz when the polymer concentration increases from 0% to 7%. This effect seems to be less dependent on the polymer network density at relatively higher temperatures $\geq T_c + 0.5$ °C (Fig. 17 (b)). Similar behaviors have been observed in the case of dispersed silica particles on FLC matrix near the SmA-SmC phase transition [6–8]. However, Kundu et al. [25] showed for other PSFLC systems that the soft-mode dielectric strength remains unchanged when the FLC cells are stabilized by a polymer network formed from a nonmesogenic reactive monomer. These authors did not provide any indications of the network structure of their systems. However Beckel et al. [44] demonstrated that nonmesogenic monomers give rise to polymer chains which microseparate from FLC molecules in the smectic layers leading to a layer swelling. Obviously, this polymer network structure is completely different to that obtained in our systems Fig. 15. In order to examine how the polymer network influences the soft-mode dielectric strength of the PSFLC, we used the model previously developed [20] to explain the electroclinic behavior of PSFLC films.

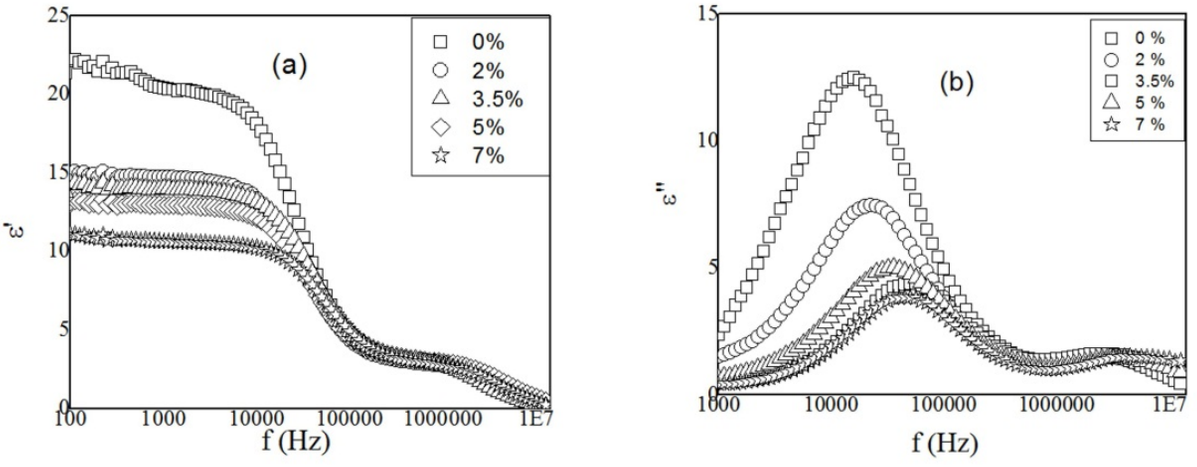

Figure 16. Frequency dependence of (a) the real and (b) the imaginary parts of the complex permittivity at the SmC-SmAphase-transition temperature, Tc, for different polymer concentrations.

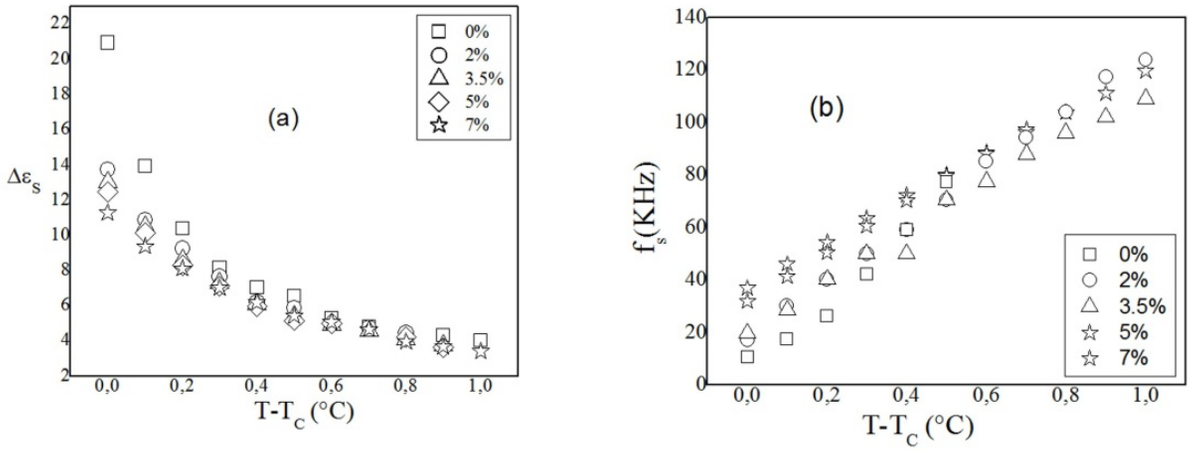

Figure 17. Temperature dependence of (a) the dielectric strength and (b) the relaxation frequency f_s of the soft mode in the smectic Aphase for different polymer concentrations.

Although polymer networks formed in liquid crystal media generally have a complex structure, they have been previously modeled as an assembly of parallel cylinders randomly distributed within the liquid crystal media [7]. The cylinders are interconnected via a chemical cross linking which ensure the network stability. In the framework of the rigid model of the network introduced by Li et al. [17], they considered that FLC molecules are affected by the bulk anchoring force from network. Li et al. interpreted this bulk anchoring force in terms of a field like effect, where the orientation of the FLC molecules was coupled to that of the anisotropic polymer network. This model gives a macroscopic description of the polymer network and was successfully applied to describe the "V-shaped" electro-optic properties of FLC gels [17]. We adopt in our theoretical approach this model structure of random polymer network of Li et al. We will consider below as a characteristic parameter of the polymer network structure the average intercylinder distance, which we call L_c, (Figure 18) and we try to analyze the effect of the applied electric field on smectic-A layers confined between two successive cylinders. The basic relation giving the free energy density of a chiral SmA phase near T_c in the presence of a small electric field E was expressed by Garoff et al. [45,46] as:

$$f_E = f_0 + (1/2)\,\alpha\,(T-T_c)\theta^2 - CP\theta + (P^2/\varepsilon_0\chi C) - PE \quad (4)$$

f_0 represents contributions to free energy density from the undistorted SmA phase. α is the mean-field coefficient and C is related to the piezoelectric coupling between the polarization P and the induced electroclinic tilt θ. ε_0 is the dielectric constant and χ is the electric susceptibility. Moreover, to the free energy density term expressed in Eq.4, two other contributions are required to describe the effect of electric field on SmA blocks confined between the polymer fibers. The first one consists of the free energy density f_{ps} arising from the bulk polymer stabilization, and may be written as [17]

$$f_{ps} = (1/2)\,W_p \sin^2\theta \approx (1/2)\,W_p\,\theta^2 \quad (5)$$

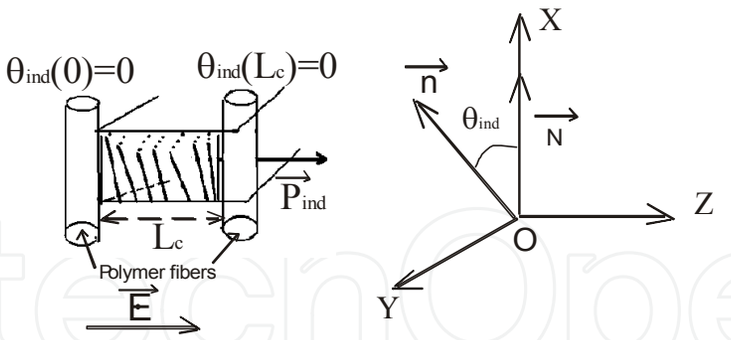

Figure 18. Tilt angle induced by electric field in the SmA* phase; distortion due to the anchorage at the polymer boundaries (on the left). L_c is the average distance between two successive polymer fibers parallel to the direction of the electric field. Cell normal and layer normal are parallel to the Z and X axis respectively.

W_p is the coupling coefficient for the interaction between the polymer network and the liquid crystal molecular director. Equation 5 is an approximative expression of f_{ps} because we are interested in low field regime where the angle is small. The second contribution comes from the elastic free energy density f_{el} arising from a director distortion upon application of E. In our system, the smectic layers are arranged perpendicular to the direction of the fibers. Between two successive groups of fibers separated by the average distance L_c (Figure18), due to anchoring forces between the liquid crystal molecules and the polymer network, the rotation of the director can be reasonably assumed not to be uniform: It is larger at or close to $L_c/2$ and weaker near the surface fibers. We must remark here that this theoretical approach of our PSFLC system is based on a one-dimensional model. We neglect then any splay deformation of the director, and we only consider the elastic energy arising from a twist deformation. f_{el} can then be given by the following expression:

$$f_{el} = (1/2)\, K_2\, (\partial\theta/\partial z)^2 \tag{6}$$

K_2 is the twist elastic constant, and Z denotes the coordinate along the axis parallel to the direction of the applied electric field. The total free energy density $f_t = f_E + f_{el} + f_{ps}$ is then expressed as :

$$f_t = f_0 + (1/2)\,\alpha\,(T-T_c)\theta^2 - CP\theta + (P^2/\varepsilon_0\chi C) - PE + (1/2)\,K_2\,(\partial\theta/\partial z)^2 + (1/2)\,W_p\,\theta^2 \tag{7}$$

The equilibrium values of P and θ are found by minimizing the free energy f_t with respect to P and θ, respectively. This leads to the following equations:

$$\alpha\,(T-T_c)\theta - CP + W_p\,\theta - K_2\,(\partial^2\theta/\partial z^2) = 0 \tag{8}$$

$$C\theta - (P/\varepsilon_0\chi) + E = 0 \tag{9}$$

Inserting Eq. 9 into Eq. 8 gives

$$K_2\,(\partial^2\theta/\partial z^2) - \alpha\,(T-T'_c)\theta + C\,\varepsilon_0\chi\,E = 0 \tag{10}$$

where $T'_c = T_c - W_p / \alpha$ is the SmC*–SmA transition temperature of the PSFLC system; $T_c = T_0 + C^2 \chi \varepsilon_0 / \alpha$ is the SmC*–SmA transition temperature of pure FLC. Equation 10 governing the director distortion induced by an applied electric field in the SmA phase the anisotropic polymer fibers in PSFLC systems constrain the molecular orientation at their surfaces as the screw dislocations at the grain boundaries in the TGBA phase do. To solve Eq. 10, we assume the anchoring of the molecules at the fiber surfaces to be rigid. The boundary conditions at these surfaces are : $\theta(z=0) = \theta(z=L_c) = 0$

Equation 10 has a solution :

$$\theta(z) = (\varepsilon \chi CE)(\alpha (T-T'_c))^{-1} [1 - \exp(z/a)((1-\exp(L_c/a))^{-1} - \exp(-z/a)(1+\exp(-L_c/a))^{-1}] \quad (11)$$

Where

$$a = (K_2/(\alpha(T-T_c))^{1/2}$$

Averaging the $\theta(z)$ [15] and $P(z)$ values over the $0 \le z \le L_c$ domain (Figure 18) gives the expression of the mean induced tilt and polarization :

$$\langle \theta^{PSFLC} \rangle = (\varepsilon_0 \chi CE)/\alpha(T-T'_c)[1 - \tanh(L_c/2a) / (L_c/2a)] \quad (12)$$

$$\langle P^{PSFLC} \rangle = (\varepsilon_0 \chi E) + (\varepsilon_0 \chi^2 C^2 E) / \alpha(T-T'_c)[1 - \tanh(L_c/2a) / (L_c/2a)] \quad (13)$$

Where

$$a = K_2 (\alpha(T-T'_c))^{-1}$$

The average induced polarization can also be written as :

$$\langle P^{PSFLC} \rangle = (\varepsilon_0 \chi E) + (\varepsilon_0 E \Delta\varepsilon^{PSFLC}) \quad (14)$$

The identification between equations (13) and (14) gives the expression of the dielectric strength of the soft mode, $\Delta\varepsilon^{PSFLC}$, as a function of L_c :

$$\Delta\varepsilon^{PSFLC} \approx (\varepsilon_0 \chi^2 C^2 E) / \alpha(T-T'_c)[1-H] \quad (15)$$

Where $H = \tanh(L_c/2a)/(L_c/2a)$ which we called the elastic parameter, depends on the network density via L_c. For a same given reduced temperature, $(T-T'_c)$, the equation (10) can be expressed as:

$$\Delta\varepsilon^{PSFLC} \approx \Delta\varepsilon^{FLC}[1-H] \quad (16)$$

$\Delta\varepsilon^{FLC}$ denotes the soft mode dielectric strength of the pure FLC. Equation (16) shows that, in the SmA* phase, the main parameter that governs the soft mode dielectric strength in the PSFLC films is L_c. This means that the stored elastic energy arising from the distortion of the director upon application of electric field is as much larger than the L_c becomes smaller, which causes a decreases of the soft mode dielectric strength (equation (16)). The effect of the polymer concentration on the dielectric strength is in accordance with the theoretical results (Equation 16). According to this equation, the $\Delta\varepsilon_s$ is reduced by the increase of the polymer network

density or by decreasing the distance L_c. To explain quantitatively the behavior of the reduction of the soft mode dielectric strength we can use the expression given by equation (16). From this equation, we conclude that the main parameter which governs the soft mode dielectric strength is the vertical distance which separated between two successive groups of polymer fibers L_c. We used the values of $\alpha \approx 8.8\ 10^{+3}\ N\ m^{-2}K^{-1}$, $a = 0.12\mu m$ [20], and the values of $\Delta\varepsilon$ presented in the Figure 17(a) at $T\text{-}T_c = 0.1°\,C$, with a reasonable value of the twist elastic constant, typically, $K_2 \approx 10^{-11}$ N, the equation (16) was graphically resolved to evaluate L_c. We obtain a mean inter-fiber L_c. The results are displayed in Fig. 15. The calculated values were compared to those directly measured from the topography of the polymer networks obtained by means of AFM experiments (Fig. 19). Figure 19 shows example of AFM images and height profiles on the z direction in Fig. 18 of the polymer network. The height profile in the **z** direction indicates two successive groups of fibers. The mean distance L_c Fig. 18 between them was evaluated for each polymer concentration and displayed in Fig. 20(a). The measured values of L_c linearly decrease with the polymer density and agree well with those calculated from the model. It seems from these results that the fibrillar and anisotropic nature of the network stabilizes, at long-range scale, the SmA order and opposes the electric field effect on the deformation of the SmA director. These results are in accordance with previous works [19,20] of the electroclinic effect in the same PSFLC systems, which demonstrate that the electroclinic susceptibility of these systems is reduced with the increase in the polymer network density. It must be noted here that the average lateral separation distance (y direction in Fig.18) between polymer strands is estimated to be about 10 μm (Fig. 19), which is 1 order of magnitude higher than L_c.

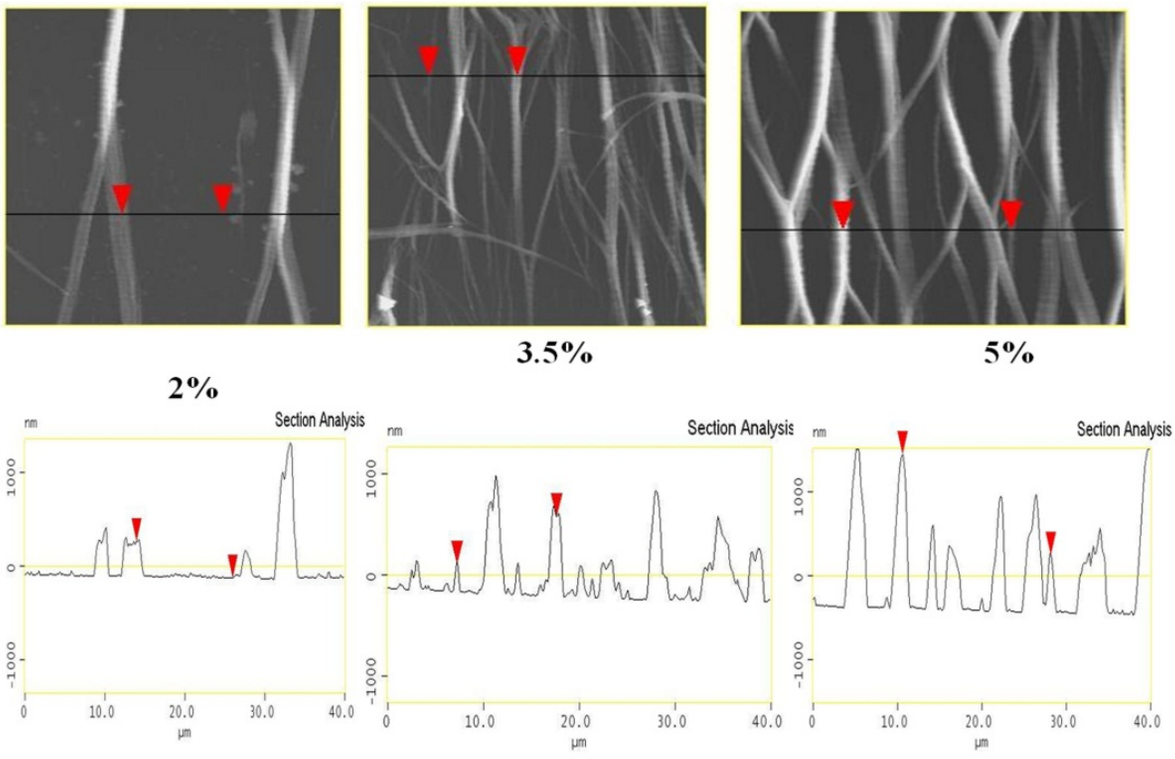

Figure 19. Tapping mode AFM images of polymer network structure of 40 x 40 μm ² (upper) and the height profile of the network structure (lower) of the 2%, 3.5% and 5%, respectively polymer concentration formed at T=25°C.

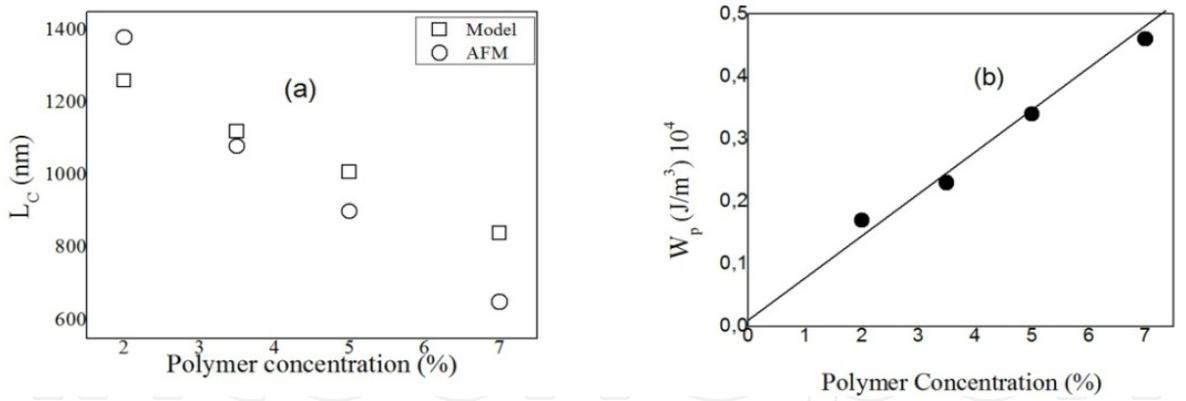

Figure 20. The average distance between two successive groups of fibers L_c as a function of polymer concentration (a) and the coupling interaction Polymer-Liquid crystals (W_P)(b).

This difference between interfiber distances in the two directions is an unexpected result. In fact, during the photopolymerization process, the mobility of the reactive monomers could be comparable within the smectic layers so that they present the same ability to come together and react to form the network. This ability could be significantly different across the smectic layers. Therefore, it would be reasonable to suspect that the average distance between polymer fibers could be of the same order of magnitude in lateral direction as well as in the z direction. The result found here is not yet clear, and the physical and chemical mechanisms governing the formation of the network could provide an explanation of our finding. This is not the aim of the work presented in this chapter. From the shift of the transition temperature, $\Delta T=T_c-T'_c = W_p/\alpha$, the coupling coefficient, W_p, characterizing the interaction energy between the FLC and the polymer network can be estimated. ΔTc values of 0.2 °C, 0.5 °C, 0.7 °C, an 0.9 °C were found for the polymer concentration of 2%, 3.5%, 5%, and 7%, respectively. The values of W_p are displayed in Fig. 20 (b). W_p linearly increases with the polymer concentration. The linear behavior of Wp in PSFLC system was already reported in earlier works [18-20]. The value of W_P found here are within 1 order of magnitude of those reported by Furue et al. [21] and Li et al. [17] on other PSFLC systems.

3.2.2. Effect of the polymer network morphology created under electric field in the short pitch ferroelectric liquid crystal on the dielectric responses

In this study we show that, both the dielectric intensity and the relaxation frequencies of the collective relaxations mechanisms namely soft and the Goldstone modes are strongly affected not only by the presence of the polymer network but also by the polymerization conditions.

Two samples cells with7% polymer concentration were then exposed to ultraviolet light (wavelength λ = 365nm) at 25 °C with an intensity of 18 (mW/cm^2) for 30 minutes. One of each is polymerized without the presence of electric field, however, the other cell is polymerized with the presence of AC electric field at $5\ V\ \mu m^{-1}$ and for $f= 1\ Hz$.

*Goldstone mode of the SmC**

In Figures 21 (a) and (b) the parameters $\Delta\varepsilon_G$ and f_G obtained from the curve-fit procedure are displayed. For all studied samples, the behavior of $\Delta\varepsilon_G$ versus temperature shows the

same general features (Figure 21 (a)). As seen in this figure, $\Delta\varepsilon_G$ increases slightly to reach a maximum at T_{max} (3°C below T_c). Above T_{max}, $\Delta\varepsilon_G$ abruptly decreases.

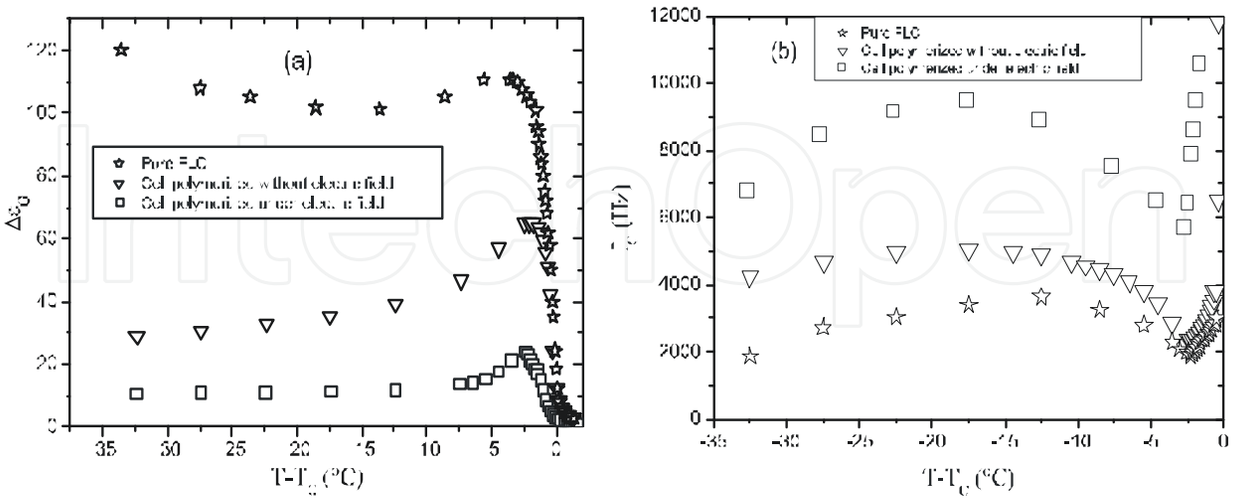

Figure 21. Temperature dependence of the Goldstone mode dielectric intensity (a) and the relaxation frequency (b).

Figure 21(b). This figure shows that the f_G slightly increases with temperature, reaches a maximum, then rapidly decreases to a minimum value at a temperature corresponding to T_{max}. It can be see from the figure 21 (b) that at room temperature, the f_G values are about 1.5 *kHz*, 4 *kHz* and 7 *kHz* for pure FLC, cell polymerized without and that polymerized with electric field, respectively. Significant differences were reported by Kaur et al [23] in another PSFLC systems. These authors were reported that the relaxation frequency f_G for the case when an bias field is applied during the polymerisation is very lower than in the case for sample when no bias was applied during the polymerisation. From the Equation (2) and (Equation 3), the values of K_{eff} are found about 2 10^{-11} N and 5.6 10^{-11} N for mixtures polymerized without and those polymerized with electric field, respectively. In conclusion, a lower dielectric strength (or larger relaxation frequency) could appear for a result of an increase of the elastic constant.

Soft mode of the SmA phase*

In Figures 22 (a) and (b) the temperature dependences of the dielectric strength, $\Delta\varepsilon_S$, and the relaxation frequencies, f_S, are shown for the soft mode detected in the SmA phase. One can see that at $(T-T_c)=0.1°$ *C*, an increase in the polymer concentration leads to the strong reduction of the soft mode dielectric strength. At the same temperature, $\Delta\varepsilon_S$ for a mixture polymerized without electric field is three times higher than those polymerized under electric field.

It can be seen that, at $T-T_c=0.1$°C, an increase of the polymer concentration from 0 to 7% leads to an increase of f_S from 10 *KHz* to 40 *KHz*, respectively. It can be seen from this figure that, at $T-T_c=0.1°$ *C* the cell polymerized with electric field presents a high f_S value about 80 *KHz (Figure 22(b)*. To explain quantitatively the behavior of the reduction of the soft mode dielectric strength we can use the expression given by equation (16). We used the values of $\alpha \approx 8.8\ 10^{+3}$ N m^{-2}K^{-1}, a =0.12μm [19,20], and the values of $\Delta\varepsilon_S$ presented in the Figure 22(a) at $T-T_c=0.1°$ *C*, with a

reasonable value of the twist elastic constant, typically, $K_2 \approx 10^{-11}$ N, the equation (16) was graphically resolved to evaluate L_c. We obtain a mean inter-fiber distance $L_c \approx 500$ *nm* and 200 *nm*, for samples polymerized without and those polymerized with electric field respectively.

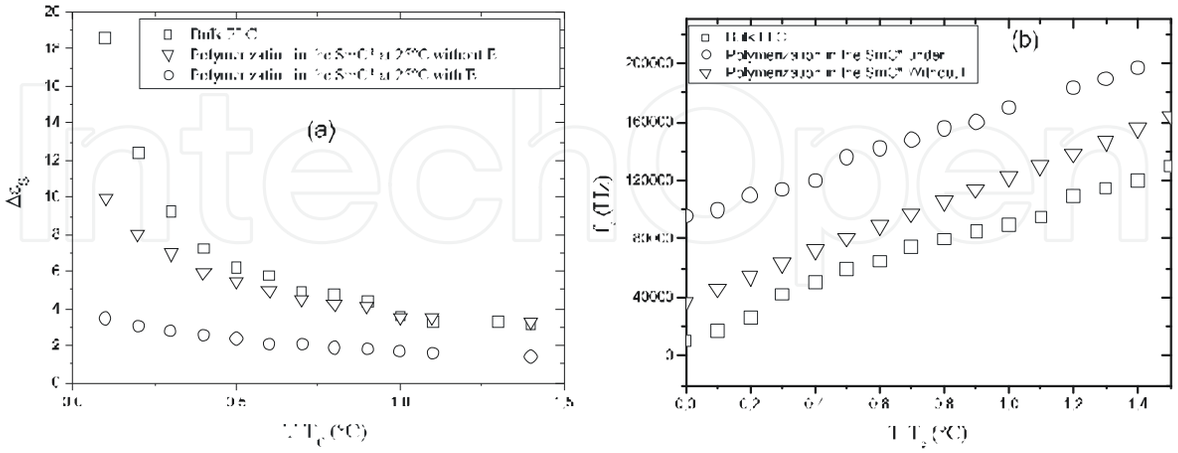

Figure 22. Temperature dependence of the dielectric intensity (a) and the relaxation frequency (b) of the soft mode in the smectic A* phase.

Atomic force microscopy observations

Figure 23 shows examples of AFM images and height profiles in the *z* direction of the Figure 18 of the polymer networks. These figures reveal that the separation distance between two polymer fibers (in the *Y* direction of the Figure 18) varies from 1 μm to 3μm for the cell polymerized without electric field and from 300 *nm* to 500 *nm* for sample polymerized under electric field. The diameter of the fibrils was found varied between 500 *nm* and 1μm for sample polymerized without electric field. However, it is found between 200*nm* and 700 *nm* for sample polymerized with electric field.

Figures 3 and 4 (lower) represent the height profiles (on the *z* direction in the figure2) of the polymer networks. The height profiles show two successive groups of fibers. The mean distance, L_c between them was evaluated for each sample and are about 480*nm* and 250 *nm* for samples when no field was applied during the polymerisation and those polymerized under electric field respectively. In conclusion, it must be noted from these observations that the polymerization under electric field is a principal factor affecting the polymer network structure. These calculated values are in accordance with those measured by the model. ΔT_c values of the sample polymerized without Electric and those polymerized with E are 0.9°C and 1.4°C, respectively. The coupling interaction W_P values are 0.46 10^4 (J/m^3) and 12,3 10^4 (J/m^3) for sample polymerized without electric field and those polymerized with electric field respectively.

In conclusion, the main parameter which governs the dielectric strength and the relaxation frequency in our PSFLC systems is the distance L_c which separated between two layers of the polymer network in the Z direction parallel to the direction of the electric field. The changes observed on the dielectric response are confirmed by AFM pictures. The polymerization under electric field is another factor affecting the structure of the polymer network formed in liquid crystals.

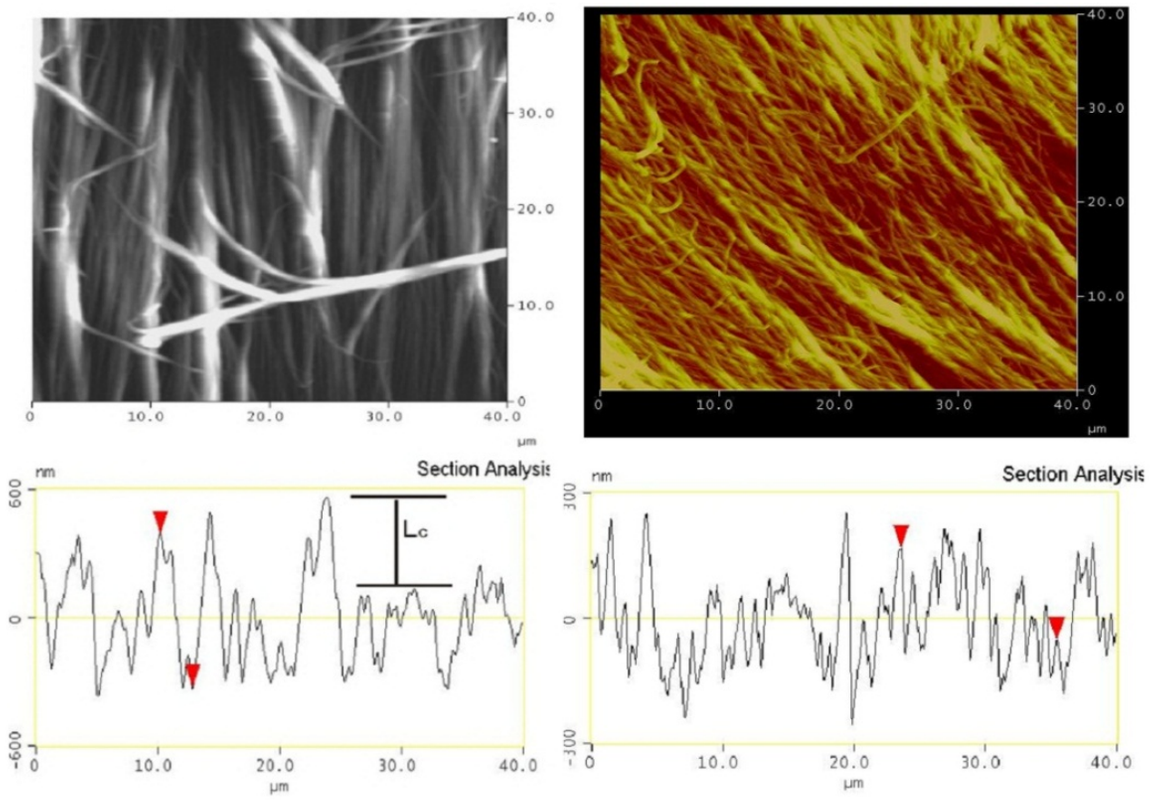

Figure 23. Tapping mode AFM images of polymer network structure of 40 x 40 µm ² (upper) and the height profile of the network structure (lower) of the 7% polymer concentration (polymerization without electric field) on the left and that polymerized under electric field (on the right).

Author details

M. Petit
Université 20 Août 1955-Skikda, Algérie

4. References

[1] Drzaic PS (1986) Polymer dispersed nematic liquid crystal for large area displays and light valves. J. Appl. Phys., 60 : 2142.
[2] Fergason JL (1985) Polymer encapsulated nematic liquid crystals for display and light control applications. SID Dig. Tech. Pap, 16, 68.
[3] Drzaic PS (1995) Liquid Crystal dispersions, World Scientific, NJ
[4] Doane JW, Vaz NA, Wu BG, Zumer S (1986) Field controlled light scattering from nematic microdroplets. Appl. Phys. Lett., 48: 296.
[5] Doane JW, Golemme A, West JL, Whitehead JB, Wu BG (1988) Polymer Dispersed Liquid Crystals for Display Applications. Mol. Cryst. Liq. Cryst., 165: 511.
[6] Broer D, Gossink R, Hikmet R.A.M (1990) Oriented polymer networks obtained by photopolymerization of liquid-crystalline monomers. Angew. Makromol. Chem. 183: 45.
[7] Crawford G.P, Zumer S. (1996) Liquid Crystals in Complex Geometries Formed by Polymer and Porous Networks (Taylor & Francis, London).

[8] Hikmet RAM, Boots HMJ, (1995) Domain structure and switching behavior of anisotropic gels. Phys. Rev. E 51: 5824-5831.
[9] Chang CC, Chien LC, Meyer RB (1997) Electro-optical study of nematic elastomer gels. Phys. Rev. E 56: 595 599.
[10] Ma RQ, Yang DK (2000) Fréedericksz transition in polymer-stabilized nematic liquid crystals. Phys. Rev. E 61: 1567-1573.
[11] Fung YK, Yang DK, Sun Y, Chien LC, Zumer S, Doane JW (1995) Polymer networks formed in liquid crystals. Liq. Cryst. 19: 797-801.
[12] Dierking I, Kosbar LL, Afzali Adakani A, Lowe AC., Held GA (1997) Two-stage switching behavior of polymer stabilized cholesteric textures. J. Appl. Phys. 81: 3007.
[13] Rajaram CV, Hudson SD, Chien LC,
[14] Doane, Chien, Yang, Bos – see chapters 1, 4, 5, 11, 12, 13 of Liquid Crystals in Complex Geometries, edited by GP Crawford & S. Zumer (Taylor & Frances, London. 1996)
[15] Rajaram CV, Hudson SD, Chien LC (1996) Effect of Polymerization Temperature on the Morphology and Electrooptic Properties of Polymer-Stabilized Liquid Crystals. Chem. Mater. 8: 2451.
[16] Dierking I, Osipov MA, Lagerwall ST (2000) The effect of a polymer network on smectic phase structure as probed by polarization measurements on a ferroelectric liquid crystal. Eur. Phys. J. E 2: 303.
[17] Li J, Zhu X, Xuan L, Huang X (2002) "V-Shaped" Electro-Optic Characteristics in FLC Gels Ferroelectrics 277: 85-105.
[18] Petit M, Daoudi A, Ismaili M, Buisine JM, (2006) Distortion and unwinding of the helical structure in polymer-stabilized short-pitch ferroelectric liquid crystal. Eur. Phys.J. E 20: 327.
[19] Petit M, Daoudi A, Ismaili M, Buisine JM, Da Costa A (2008) Effect of the Polymer Network Density Formed in Short Pitch Ferroelectric Liquid Crystal on the Electroclinic Effect Mol. Cryst. Liq. Cryst. 487: 61-73.
[20] Petit M, Daoudi A, Ismaili M, Buisine JM (2006) Electroclinic effect in a chiral smectic- *A* liquid crystal stabilized by an anisotropic polymer network .Phys. Rev. E 74: 061707.
[21] Furue H, Takahashi T, Kobayashi S (1999) Monostabilization of Surface-Stabilized Ferroelectric Liquid Crystal Using Polymer Stabilization. Jpn. J. Appl. Phys., Part 1 38: 5660-5663.
[22] Takahashi T, Umeda T, Furue H, Kobayashi S (1999) Modeling and Computer Simulation of the Electrooptic Response of Polymer-Stabilized Ferroelectric Liquid Crystal Cells. Jpn. J.Appl. Phys., Part 1 38: 5991-5995.
[23] Kaur S, Dierking I, Gleeson HF (2009) Dielectric spectroscopy of Polymer Stabilised Ferroelectric Liquid Crystals. *Eur. Phys. J. E*, 30: 265-274.
[24] Mukherjee A, Bhattacharyya SS, Chaudhuri BK, Wu SL (2009)Effect of polymer relaxation on dielectric spectroscopic study of polymer–ferroelectric liquid crystal composites. *Journal of Molecular Liquids*, 148, 127,
[25] Kundu S, Ray T, Roy SK, Haase W, Dabrowski R (2003) Effect of UV Curable Polymer on The Dielectric & Electro-Optic Properties of Ferroelectric Liquid Crystal. *Ferroelectrics*. 282, 239-248
[26] Petit M, Hemine J, Daoudi A, Ismaili M, Buisine JM, Da Costa A (2009) Effect of the network density on dynamics of the soft and the Goldstone modes in short-

ferroelectric liquid crystals stabilized by an anisotropic polymer network .*Phys. Rev. E*, 79, 031705-9
[27] Blinc R, Zeks B (1978) Dynamics of helicoidal ferroelectric smectic-$C^{\sim}$ liquid crystals. Phys. Rev. A.18. 740-745.
[28] Goodby JW et al.∴Ferroelectric Liquid Crystals: Principales, Properties and Applications. (Gordon and Breach Science Publishers 1991)
[29] Musevic I, Blinc R, Zeks B (200)The Physics of Ferroelectric and Antiferroelectric Liquid Crystals.(World Scientific).
[30] Glogarova M, Pavel J (1984) The Behaviour of Thin Samples of Ferroelectric Liquid Crystals. Mol. Cryst. Liq. Cryst 114, 249-257.
[31] Brunet M, Parodi O (1982)Défauts dans les smectiques C chiraux. - II- Double paroi de déchiralisation, J. Phys. France 43, 515-522.
[32] Bouligand Y (1975) Defects and Textures in Cholesteric Analogues Given by Some Biological Systems *J. Phys*., 36, C1-331.
[33] Archer P, Dierking I (2009) Polymer stabilisation of twisted smectic liquid crystal defect states *Soft Matter*, 5, 835.
[34] Baytch N, Selinger RLB, Selinger JV, Shashidhar R (2003) Simulations of helix unwinding in ferroelectric liquid crystals.Phys. Rev. E. 68, 041702.
[35] M. Gasser, A. Gembus, D. Ganzke, and I. Dierking (2000) Collective dynamics of polymer-network stabilized ferroelectric liquid crystals. Mol. Mater. 12, 347.
[36] Kutnjak Z, Kralj S, Žumer S (2002)Effect of dispersed silica particles on the smectic-*A*–smectic-C^* phase transition.Phys. Rev. E 66, 041702.
[37] Rozanski SA, Thoen J (2005) Influence of dispersed aerosil particles on the collective dynamic modes in a ferroelectric liquid crystal with polarization sign reversal Non-Cryst. Solids 351, 2802.
[38] Rozanski SA, Thoen J (2005) Collective dynamic modes in ferroelectric liquid crystal-aerosil dispersions. Liq. Cryst. 32, 331-340 2005.
[39] Carlsson T, Zeks B, Filipic C, Levstik A (1990) Theoretical model of the frequency and temperature dependence of the complex dielectric constant of ferroelectric liquid crystals near the smectic-C^*–smectic-*A* phase transition. Phys. Rev. A 42, 877-889.
[40] Held GA, Kosbar LL, Dierking I, Lowe AC, Grinstein G, Lee V, Miller RD (1997) Confocal Microscopy Study of Texture Transitions in a Polymer Stabilized Cholesteric Liquid Crystal. Phys. Rev. Lett. 79, 3443-3446.
[41] Goh M, Kyotani M, Akagi K (2007) Highly twisted helical polyacetylene with morphology free from the bundle of fibrils synthesized in chiral nematic liquid crystal reaction field. *J. Am. Chem. Soc.*, 129 (27), 8519 -8527.
[42] Hoischen A, Benning SA, Kitzerow HS(2009) Electroconvection of liquid crystals: Tool for fabricating modulated polymer surfaces. J. Appl. Phys. 105, 013540.
[43] Kaur S, Dierking I, Gleeson HF(2009). Eur. Phys. J. E, 2, 3, (2009).
[44] Beckel E, Cramer NB, Harant AW, Bowman CN (2003) Electro-optic properties of thiol-ene polymer stabilized ferroelectric liquid crystals. Liq. Cryst. 30, 1343.
[45] Garoff S, Meyer RB (1977) Electroclinic Effect at the *A*-*C* Phase Change in a Chiral Smectic Liquid Crystal.Phys. Rev. Lett. 38, 848-851.
[46] Garoff S, Meyer RB (1979) Electroclinic effect at the *A*-*C* phase change in a chiral smectic liquid crystal. Phys. Rev. A 19, 338-347.